

Structural and morphological evolution of powders nanostructured ceramics: transitional aluminas

L. Fillali^{1,2}, S. López-Andrés², A. López-Delgado¹, I. Padilla¹, and J.A. Jiménez¹

¹National Center for Metallurgical Research. CSIC. ES-28040. Madrid. Spain

²Dpt. Crystallography and Mineralogy, Faculty of Geology. UCM. ES-28040. Madrid. Spain

Abstract. This work aims with the study of the transformation of boehmite into transitional aluminas. Boehmite was obtained by a sol-gel method from an aluminium hazardous waste. The thermal behaviour of boehmite was followed by thermogravimetry and differential thermal analysis to determine the transformation temperatures. By calcinations of boehmite at temperatures ranging between 250-1000°C, transitional aluminas (γ , δ , θ -Al₂O₃) were synthesized and characterized by XRD, TEM and FTIR. All the transitional aluminas exhibit nanometric crystallite size, ranging from 2.5-15nm. γ -Al₂O₃ was obtained as a nanostructured material at 500 °C with a cell parameter $a=7.923\text{Å}$. δ -phase starts to appear at 850 °C with a crystallite size of 6nm and cell parameters $a=5.672\text{Å}$ and $c=24.600\text{Å}$. For θ -Al₂O₃ the cell parameters, in Å, were $a=11.817$, $b=2.912$, $c=5.621$ and $\beta=103.8^\circ$. The progressive conversion of the transitional phase γ -Al₂O₃ into the stable polymorph α -alumina, takes place gradually and a four-phases region is achieved at 1000°C, where coexist with other transitional phase such as δ - and θ -Al₂O₃.

1 Introduction

Alumina is a ceramic widely used for its mechanical, thermal and electric insulation properties. Many studies have focused on the structural study of alumina, given their applications in various industries such as ceramics, cement, abrasives, paint manufacturing, catalysts and catalyst support [1,2]. The catalytic properties of aluminium oxides depend largely on crystalline structure and textural properties [3,4]. Several processes to obtain this type of solid have been cited in the literature, such as thermal evaporation methods [5], chemical engraving [6], sol-gel methods [7], and continuous anodizing [8].

Different types of aluminas can be obtained from the dehydration of aluminium hydroxides as boehmite and pseudoboehmite. In previous paper, the transformation of boehmite into corundum was studied [9]. The main goal of the present paper is to study the structural and morphological evolution of boehmite into transitional aluminas by FTIR, TEM and XRD. The alumina precursor, boehmite, used in this paper was synthesized from a hazardous waste coming from tertiary aluminium industry employed a sol-gel method [10].

2 Experimental procedure

2.1. Synthesis

A sample of 20g of Al-containing waste was subjected to acid digestion consisting of dissolving soluble aluminium compounds in HCl (10% v/v) during 150min. The Al-containing waste employed in this work came from the Al-dross milling operation and was supplied by a tertiary aluminium industry

(Recuperaciones y Reciclajes Roman S.L. Fuenlabrada, Madrid, Spain).

The major mineralogical composition of the waste (expressed wt%) is as follows: 31.2 Al metal, 20.0 corundum, 15.0 spinel, 8.4 aluminium nitride, 8.0 quartz, 8.2 calcite, 1.8 hematite, 1.5 titanium dioxide, 1.5 sodium/potassium chloride, 0.7 aluminium sulphide and other minor metal oxides.

The pH of the resulting solution from the acid digestion step was increased by adding NaOH solution (1M) up to pH 8. A massive gelification took place around pH 6 and the emulsion was kept stirring for 24h. Gel was dried at 150 °C for 24h, and then crushed to get a fine powder. The as-obtained xerogel was calcined in a furnace for 7h at different temperatures from 250 to 1000 °C.

2.2. Characterization

The thermal transformation of boehmite into alumina was followed by simultaneous thermogravimetry and differential thermal analysis (TG/DTA) in a TA Instrument model SDT-Q 600. Analyses were performed in N₂ atmosphere, up to 1300 °C, at a heating rate of 20 °C/min.

The chemical composition of samples was determined by X-ray fluorescence (FRX) in a Panalytical model Axios equipment. X-ray diffraction (XRD) analyses were carried out in a Siemens D 5000 diffractometer (40 kV, 30mA) with Cu_{K α} radiation. Data was collected in the 2 θ angle range of 20–100 ° at a rate of 2 °/min. Transmission electron microscopy (TEM) observations were performed in a Joel JEM-2100 equipment at 200KeV. Samples were prepared by ultrasonic dispersion of powder in acetone, and then applying a drop on polymeric coated copper grid. High resolution imaging was performed to analyze the

crystalline quality of samples. Selected areas of electron diffraction were used to elucidate the presence of amorphous phase and crystalline structure. Fourier-transformed infrared (FTIR) spectra were recorded on sample/CsI discs, in the 1300-250 cm^{-1} range (Nicolet Magna-IR 550 spectrophotometer).

3 Results and discussion

The thermal behaviour of the obtained boehmite, $\text{AlOOH} \cdot 0.8\text{H}_2\text{O}$ was followed by TG and DTA. Results are shown in Table 1. The thermal process occurs in four steps with a total mass loss of 34.4% (wt) [9,10]. Differences with to previous papers are related to the hydration degree which is a consequence of the raw material and the synthesis procedure.

According to the thermal behaviour γ -alumina can be obtained at temperature close to 500 $^{\circ}\text{C}$. Nevertheless the dehydroxylation reaction does not occur through a well-defined step, and so the mass loss takes place along a wide temperature range [11].

Table 1. TG and DTA analysis of the alumina precursor.

Effect		1 endo	2 endo	3 endo	4 exo
DTA	T_{range} ($^{\circ}\text{C}$)	100-350	363-460	488-798	1093-1243
	T_{Peak} ($^{\circ}\text{C}$)	234	402	803	1221
	Peak Area ($\mu\text{V s/mg}$)	283.3	2.24	94.1	29.9
TG	T_{range} ($^{\circ}\text{C}$)	50-226	226-476	476-993	993-1287
	Mass loss (wt.%)	13.7	16.9	3.8	0

The chemical analysis of samples is presented in Table 2. It is observed an increasing in the percentage of aluminium oxides with temperature from 56.4% for sample obtained at 250 $^{\circ}\text{C}$ to 88.6% for sample at 600 $^{\circ}\text{C}$. For higher temperature, it was observed a slight increasing of Al_2O_3 content (90.6%) which is attributable to the loss of OH groups which remained into structure.

Table 2. XRF results of samples obtained at 250, 500, 600, 850 and 1000 $^{\circ}\text{C}$ for 7h (expressed as oxide wt.%).

Compounds	Calcinations temperature ($^{\circ}\text{C}$)				
	250	500	600	850	1000
(wt.%)					
Al_2O_3	56.4	88.2	88.6	90.4	90.6
Fe_2O_3	1.7	3.3	3.6	3.7	3.7
SiO_2	1.5	3.1	2.0	2.3	1.7
ZnO	0.5	1.1	0.9	1.0	0.9
P_2O_5	0.1	0.1	0.2	0.1	0.2
MgO	0.3	0.4	0.5	0.4	0.4
CaO	0.6	1.2	1.3	1.1	1.0
MnO	0.1	0.4	0.3	0.4	0.5
H_2O	35.0	-	-	-	-

3.1 XRD Characterization

Figure 1 shows the XRD patterns of samples obtained from boehmite heat treated at 250, 500, 600, 850 and 1000 $^{\circ}\text{C}$. The pattern of sample calcined at 250 $^{\circ}\text{C}$ shows the profile of boehmite (JCPDS 01-088-2112), with but very broad peaks and significant background. This indicates the starting of boehmite structure decomposition, a certain amorphization degree and very small crystallite size (2.5nm). According to thermal analysis, at this temperature, only absorbed and/or interlayer water is lost by forming the anhydrous phase AlOOH .

At 500 $^{\circ}\text{C}$, the crystalline phase identified is γ - Al_2O_3 (JCPDS 29-0063) The XRD profile indicates that this phase is composed of small size of crystallites. A similar pattern is obtained for the sample calcined at 600 $^{\circ}\text{C}$, although the intensity of the diffraction peaks is higher in this case, indicating a higher degree of crystallinity, or a larger crystallite size. The presence of other crystalline phases is not observed. The assigned hkl indexes for this phase are 120, 311, 222, 400 and 440, with a very slight shift towards higher values of the 2θ for γ - Al_2O_3 obtained at 600 $^{\circ}\text{C}$.

For sample obtained at 850 $^{\circ}\text{C}$, better defined and higher intensity diffraction peaks are observed for γ phase. Reflexions corresponding to the polymorph δ -phase (JCPDS 46-1131) are also observed. A crystallite size of 6nm was determined calculated for this at this temperature. As temperature increases, other polymorphs of alumina start to appear. Thus, at 1000 $^{\circ}\text{C}$, the transitional phase θ - Al_2O_3 (JCPDS 23-1009) and the stable α - Al_2O_3 (JCPDS 46-1212) are identified along with the previous phases. It is notice that reflections corresponding to α - Al_2O_3 are narrow and well defined, indicating high degree of crystallinity.

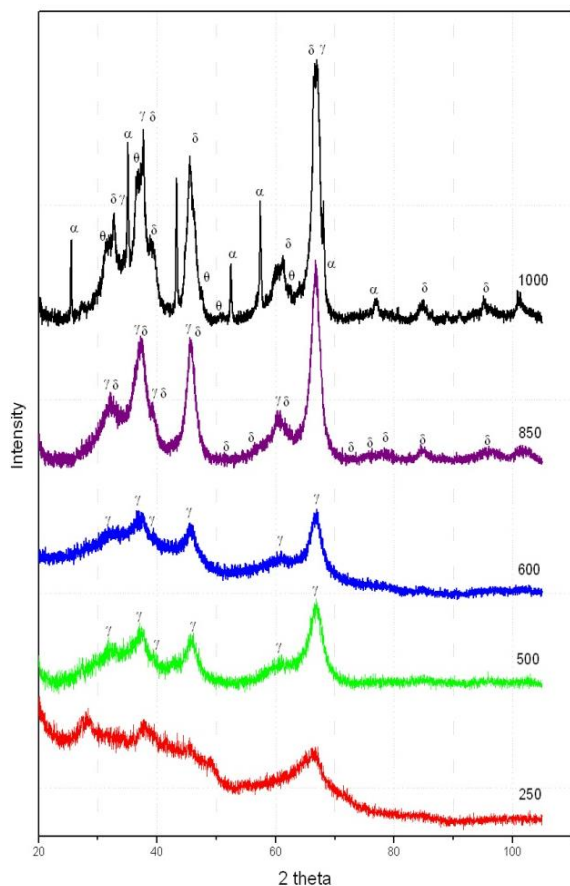


Fig.1. XRD patterns of samples obtained at 250, 500, 600,850 and 1000 °C.

The polymorphic transformation of γ phase in which Al atom is occupying tetrahedral sites, AlO_4 , towards the stable α phase, with Al atoms in octahedral site, AlO_6 , occurs through the formation of other transitional polymorphs δ - and θ -, where Al atoms are sited in both tetra- and octahedral positions. The cell parameters and the crystallite size of the different alumina phases are collected in Table 3.

Table 3. Cell parameters and crystallite size for transitional aluminas obtained by calcinations of boehmite at different temperatures.

Temperature °C		γ	δ	θ	α
		Cell parameter (Å)			
500	a	7.923			
600	a	7.924			
850	a	7.918	5.672		
	c		24.600		
1000	a	7.918	5.672	11.817	4.765
	b			2.912	
	c		24.729	5.621	13.004
	β (°)			103.8	
Crystallite size (nm)					
500		2.5			
600		3			
850		4	6		
1000		5	9	15	60

All the transitional aluminas exhibit nanometric crystallite size, ranging from 2.5-15nm. For γ - Al_2O_3 a slight increasing of size is observed as temperature increases. At 1000°C, δ and θ - Al_2O_3 have higher size than γ - Al_2O_3 . The crystallite size of corundum phase is higher than that corresponding to the transitional phases.

3.2 Infrared study

Fig. 2 shows the FTIR spectra of samples calcined at the different temperature studied, in the wavenumber region from 1300-250 cm^{-1} ; the vibrational mode Al-O which can identified the alumina polymorphic transformation are observable in this spectrum region [12].

For sample obtained at 250 °C, the vibrational modes of boehmite corresponding to both the deformation and the stretching mode of AlO_6 and AlO_4 groups appear between 300 and 400 cm^{-1} . In this case only a shoulder at 360 cm^{-1} is observed, this indicating the collapse of the boehmite structure. Bands at 603, 720, 840 and 1075 cm^{-1} can be attributable to ν_6 , ν_5 , ν_4 and ν_2 of boehmite [9].

Regarding the samples obtained at 500 and 600 °C, spectra show a broad unresolved band between 300 and 900 cm^{-1} , frequently observed for transitional alumina. Despite the poor definition several maximum values can be distinguished at the surrounding of 600, 720 and 830 cm^{-1} , correspond to stretching and bending modes of AlO_4 tetrahedral groups of γ - Al_2O_3 [13-15].

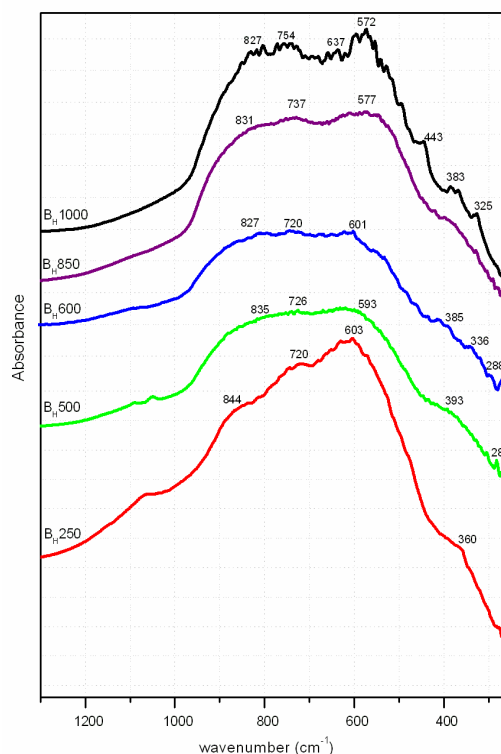


Fig. 2. FTIR spectra of samples obtained at 250, 500, 600, 850 and 1000 °C for 7h.

The FTIR spectrum corresponding to sample obtained at 850 °C exhibits several shoulder in the lowest region attributable to bending modes Al-O bonds in the AlO_6 group.

For sample obtained at 1000 °C, a higher number and better defined bands are observed, in agreement with the XRD results. Thus the typical vibrational modes of $\alpha\text{-Al}_2\text{O}_3$ are observed at 383 and 443, 572 and 637 cm^{-1} and they correspond to bending (lowest ones) and stretching (highest ones) modes of Al-O bonds in the AlO_6 group of the rhombohedral coordination [17].

3.3 Transmission electron microscopy

Fig.3 (a) presents the TEM image of γ -alumina obtained from boehmite precursor, heat treated at 500 °C for 7 hours. Aggregates of very small size (>10nm) and very thin particles with poor developed edges can be observed. The electron diffraction (image in the upper left corner of Fig. 3) shows a typical pattern of low crystallinity or polycrystalline materials. A high resolution TEM image (Fig. 3 b) shows several crystallographic planes.

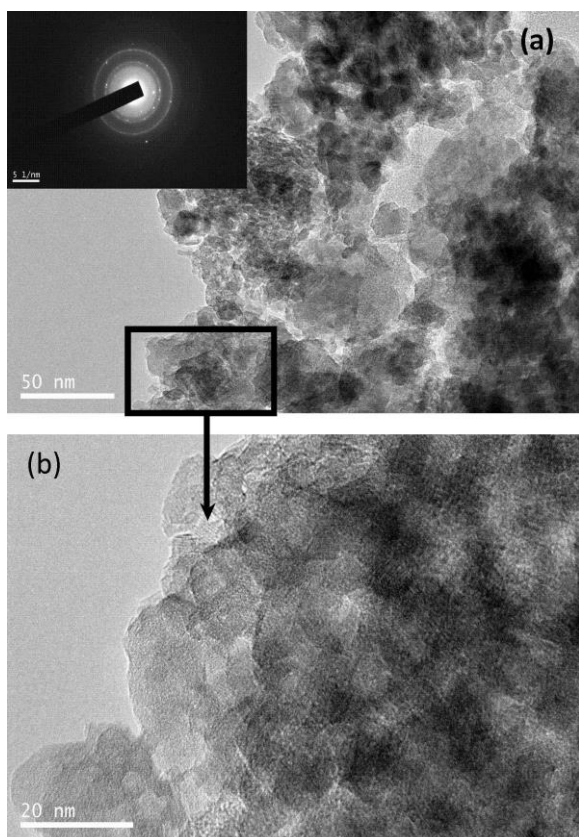


Fig. 3. TEM of $\gamma\text{-Al}_2\text{O}_3$ obtained by calcinations of boehmite at 500 °C. (a) Image of an aggregate with the corresponding electron diffraction. (b) High resolution TEM image of the marked zone.

Figure 4 shows the morphology of sample obtained at 850 °C. Although remarkable differences are not observed with respect to sample obtained at lower

temperature, several crystallites present more rounded edges which could be attributable to different transitional alumina phases [17]. The electron diffraction pattern showed in the upper left corner, indicates a polycrystalline material or of very low crystallinity. In this sample crystallographic planes are clearly observed for particle of size smaller than 10 nm.

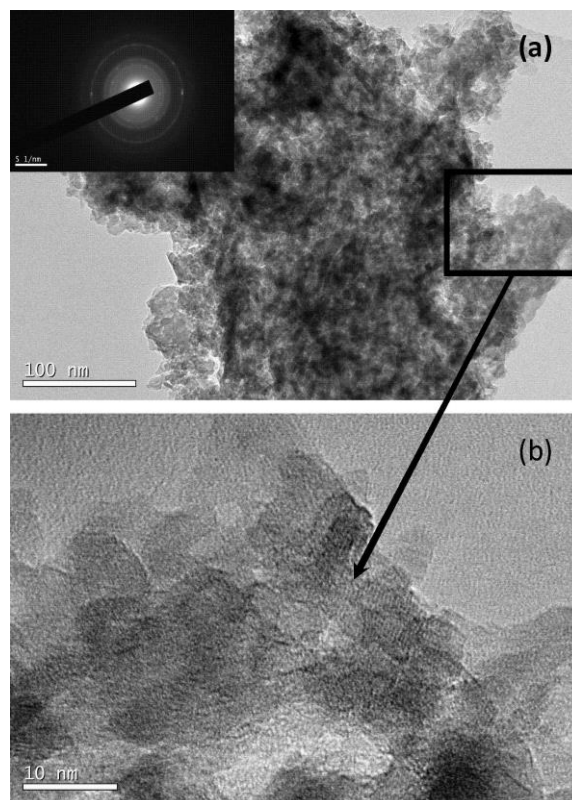


Fig.4. TEM images of sample obtained at 850 °C. (a) Image of an aggregate with the corresponding electron diffraction. (b) High resolution TEM image of the marked zone.

For sample obtained a 1000 °C, various types of morphologies can be observed (Fig. 5). Thus a grain of ~75 nm with a pseudo-hexagonal morphology, as showed in the electron diffraction pattern at the upper left corner, is attributed to α -alumina. The crystal size of this phase is similar to that obtained by XRD. The transitional aluminas (γ , δ and θ) show morphologies similar to those of phases obtained at lower temperatures: small crystallite size, thin particles and poor developed edges.

TEM results for samples obtained at all the temperature studied fit well with the crystallographic data obtained by XRD.

Conclusions

The transitional aluminas γ , δ , $\theta\text{-Al}_2\text{O}_3$ were obtained from boehmite by calcinations at different temperature in air atmosphere. All of them present nanometric crystallite sizes which slightly increase with temperature. The phase γ was obtained as unique

crystalline phase at 500 °C, and it remains at 600 °C. For higher temperature several transitional phases coexist. δ -Al₂O₃ and θ -Al₂O₃ appear at 850 and 1000 °C respectively. The progressive conversion of the transitional phase γ -Al₂O₃ into the stable polymorph alpha, takes place gradually and a four-phases region is achieved at 1000 °C, where coexist with other transitional phase such as δ - and θ -Al₂O₃.

These results allow to using a hazardous waste as a raw materials to synthesize both, alumina precursor, boehmite, and different transitional alumina with nanometric crystallite size depending on the experimental conditions.

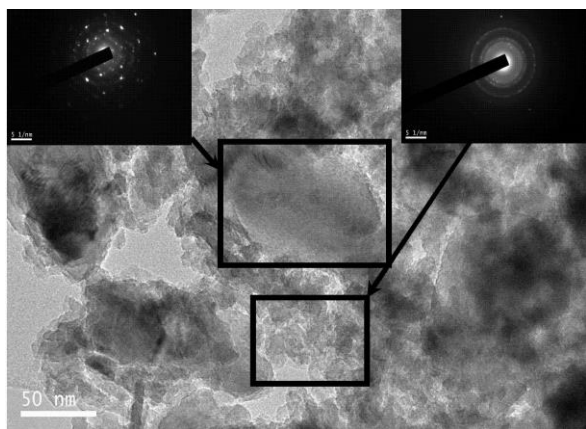


Fig.5. TEM image of sample obtained from boehmite calcined at 1000 °C. In the left and right upper corners the electron diffraction images of the marked zones.

Acknowledgment

The authors thank the company Recuperaciones y Reciclajes Roman S.L. (Fuenlabrada, Madrid, Spain) for supplying the waste. This work is sponsored by the Comisión Interministerial de Ciencia y Tecnología (CICYT), Spain, under Grants MAT2012-39124 and CTM2012-34449.

References

1. J. Sanchez-Valente, X. Bokhimi, J.A. Toledo. *App. Catal. A: General* **264**, 175 (2004).
2. P. Souza Santos, H. Souza Santos, S.P. Toledo. *Materials Research* **3**, 104 (2000).
3. Y. Kim, C. Kim, P. Kim, J. Yi, J. Non-Cryst. Solids **351**, 550 (2005).
4. B. Xu, T. Xiao, Z. Yan, X. Sun, J. Sloan, L. Gonzalez-Cortes, F. Alshahrani, M.L.H. Green, *Micr. Mesop. Mater.*, **91**, 293 (2006).
5. J. Proost, S. Van Boxel. *J. Mater. Chem*, **14**, 3058 (2004).
6. Z.L. Xiao, C.Y. Han, U. Welp, H.H. Wang, W.K. Kwok, G.A. Willing, J.M. Hiller, R.E. Cook, D. J. Miller, G.W. Crabtree, *Nano Lett.*, **2**, 1293 (2002).
7. G. Teoh, K. Liew, W. Mahmood, *J. Sol-Gel Sci. Technol.* **44**, 177 (2007).
8. W. Lee, R. Scholz, U. Gösele, *Nano Lett.* **8**, 2155 (2008).

9. A. López-Delgado, L. Fillali, J.A. Jiménez, S. López-Andrés, *J. Sol-Gel Sci. Technol.* **64**, 162 (2012).
10. L. Gonzalo-Delgado, A. López-Delgado, F.A. López, F.J. Alguacil, S. López-Andrés, *Waste Manage. Res.* **29**, 127 (2011).
11. K.J.D. MacKenzie, J. Temuujin, M.E. Smith, P. Angerer, Y. Kameshima, *Thermochim. Acta*, **359**, 87 (2000).
12. R. Rinaldi, U. Schuchardt, *J. Catal.* **236**, 335 (2005).
13. J. M. Saniger, *Mater. Lett.* **22**, 109 (1995).
14. J. M. Saniger, N.A. Sanchez, J. O Flores, *J. Fluorine Chem.* **88**, 117 (1998).
15. P. H. Colombari, *J. Mater. Sci. Lett.* **7**, 1324 (1988).
16. Z. Lodziana, K. Parlinski, *Phys. Rev. B* **67**, 174106 (2003).
17. K. Wefers, C. Misra, *Alcoa Technical Paper No. 19*. Alcoa Laboratories, Pittsburgh, PA, 1987.